

Classification of Air Clathrates Found in Polar Ice Sheets

By Frank Pauer¹, Sepp Kipfstuhl¹, Werner F. Kuhs² and Hitoshi Shoji³

Summary: Air clathrates in polar ice sheets exist in different shapes and sizes. For the description of transition states from air bubbles to clathrates and between different stages of transformation, and for statistical purposes, a classification into different categories is necessary. We have tried to establish a framework for the classification of clathrates employing criteria such as transparency, to distinguish between different stages of crystallisation, of size, to reconstruct segregation processes, and shape, to investigate the crystal properties and the processes of recrystallisation. A miscellaneous category accounts for mixed-type clathrates, which are the result of different factors leading to their formation.

Zusammenfassung: Luftclathrate in polaren Eisschilden weisen verschiedene Formen und Größen auf. Für die Beschreibung von Übergangszuständen von Luftblasen zu Clathraten und zwischen verschiedenen Transformationsphasen sowie für statistische Auswertungen ist eine Klassifizierung in verschiedene Kategorien notwendig. Ausgehend von Unterscheidungskriterien wie Transparenz, um zwischen verschiedenen Kristallisationsphasen zu unterscheiden, Größe, um Teilungsprozesse nachzuvollziehen, und Formen, um die Kristalleigenschaften und Umkristallisierungsprozesse zu untersuchen, haben wir ein Kriterienschema zur Klassifizierung von Clathraten aufgestellt. Eine weitere Kategorie beschreibt Clathrate, die verschiedenartige Merkmale auf Grund von verschiedenen Faktoren, die zu ihrer Entwicklung geführt haben, aufweisen.

INTRODUCTION

Many studies on air clathrates (also termed "air hydrates" because of their composition of a cage-like arrangement of water molecules and guest molecules occluded in the individual cages of the host lattice) in polar ice sheets have been the focus of attention since their postulation by MILLER (1969) and their discovery in 1982 (SHOJI & LANGWAY). Clathrates form from air bubbles and the surrounding ice (Ih) phase as a cage-like arrangement of H₂O molecules and individual gas molecules occluded in the cages. The temperature-pressure equilibrium line for air clathrates was inferred from those for nitrogen and oxygen clathrates by MILLER (1969).

However, for clathrate formation, an excess gas pressure must be attained before nucleation occurs. Thus, a long range of coexistence of air bubbles and clathrates is observed in polar ice cores, e.g. 700–1300 m of depth in the GRIP ice core, before all air bubbles are converted into clathrates (HONDOH 1996).

Nitrogen, oxygen, and air clathrates adopt the type II structure according to the v. Stackelberg classification (v. STACKELBERG

& MÜLLER 1958). In statistical studies, clathrates have been classified into spherical, oval, irregular, rod-like, faceted, and polyhedral categories (UCHIDA et al. 1994, PAUER et al. 1999, NARITA et al. 1999). Yet the criteria for their classification into different categories are sometimes arbitrary, as often a clear-cut distinction does not exist, as is the case between spherical and oval, oval and rod-like, or faceted and polyhedral. Primary clathrates are divided in subcategories according to the predominant feature. We have tried to find archetypal shapes of clathrates to facilitate the establishment of criteria for their distinction and classification.

The classification of clathrates is somewhat compounded not only by the overlap of different categories, but also by the fact that clathrates undergo processes that change their original shape and appearance considerably. At a shallower depth level, we mostly encounter clathrate specimens with a rough surface, which often shows signs of grooves or splintering and appear opaque, or rather translucent, in transmitted light. These clathrates often split up, forming smaller specimens (segregation), or undergo metamorphosis, the result of which are more transparent, often faceted specimens (the outlines of an overlapped clathrate can be seen). It can be assumed that clathrates that have formed as a result of segregation also metamorphose, although we have not found clear-cut examples to date. This is why we distinguish between original translucent clathrates, which we have termed "primary clathrates", and clathrates as products of metamorphosis, which we call "secondary clathrates" (KIPFSTUHL et al. 1999). It should be pointed out that this paper is concerned with the classification of clathrates according to their appearance rather than the processes leading to different shapes.

EXPERIMENTAL SECTION

Most of the observations were carried out one hour after core retrieval at ambient temperatures of –30 °C at the beginning and –20 °C at the end of the drilling season at the NGRIP drilling site (75 °N, 42 °W). The samples, about 3–25 cm in length, were frozen on glass plates and a flat surface was prepared by a microtome. Silicon oil was applied on the surface to facilitate the observation of clear images. The microscopic observations were digitally recorded on video tape and computer. Samples were taken in 25–30 m increments with additional takes in between. Clathrates were optically identified employing the Becke test (SHOJI & LANGWAY 1982). The way all these structures decompose is unique and completely different from e.g. collapsing

¹ Alfred-Wegener-Institut für Polar- und Meeresforschung, Columbusstraße, 27568 Bremerhaven, Germany

² Mineralogisch-Kristallographisches Institut der Universität Göttingen, Goldschmidtstraße 1, 37077 Göttingen, Germany

³ Kitami Institute of Technology, Department of Civil Engineering, 165 Koen-cho, Kitami 090-8507, Japan

plate-like inclusions and therefore provide additional evidence that the presented structures are air clathrates.

PRIMARY CLATHRATES

After a nucleation period, the pressure-temperature conditions in polar ice sheets lead to the formation of air clathrates, presumably starting on the bubble-ice interface (HONDOH 1996). Diffusion processes of water molecules through the clathrate shell covering the interface after nucleation have been considered necessary for the growth of the clathrate lattice towards the centre (SALAMATIN et al. 1998), but recent investigations on synthetic clathrates have suggested that the structure of the clathrate might be mesoporous (KUHS et al. 1999). This would imply that water and gas molecules could penetrate through the permeable pores of the pre-existing clathrate phase to enable clathrate growth at a presumably much greater rate than in diffusion processes through bulk ice.

This model of clathrate formation and growth suggests that the original shape of the bubble is retained, although at the depth of clathrate nucleation and formation the air in the bubble would take a greater volume (ca. 65 % more at a depth of 900 m and a temperature of $-25\text{ }^{\circ}\text{C}$) than a clathrate containing the same amount of air. The volume compression under hydrostatic pressure might account for the roughness and the grooves in the clathrate surface.

In this group, we classify the clathrates resulting from the phase transformation of air bubbles as a succession of the evolutionary stages.

1) Bubble-shaped clathrates: round and oval

The clathrate from 916 m depth in Figure 1 has a diameter of ca. $200\text{ }\mu\text{m}$, which corresponds to the order of magnitude of that of an average air bubble. Its surface is uneven and displays pits and grooves. We also find specimens with more ellipsoidal shapes, but in most cases, coherent structures without any signs of fractures prevail at shallower depths.

2) Clathrates with grooves (irregular clathrates)

Deeper down, the surface of many clathrate is rougher and contains grooves (total length of the clathrate in Fig. 2 ca. $250\text{ }\mu\text{m}$). These clathrates are often termed "graupel-like" in the literature (SHOJI & LANGWAY 1982).

3) Splintered clathrates

The next step in the segregation process is a clathrate that shows clear signs of individual splinters, which are spatially still linked to and often overlap one another.

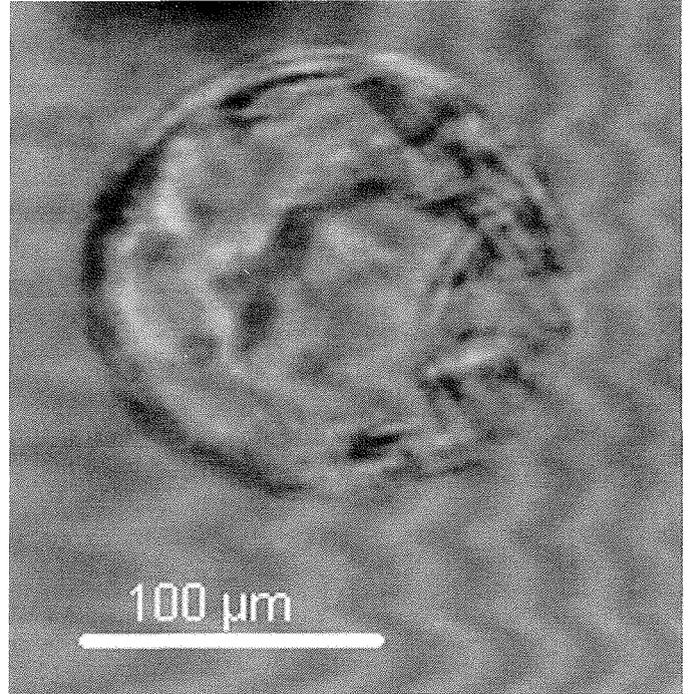


Fig. 1: Round primary clathrate (depth: 916 m).

Abb. 1: Rundes primäres Clathrat (Tiefe: 916 m).

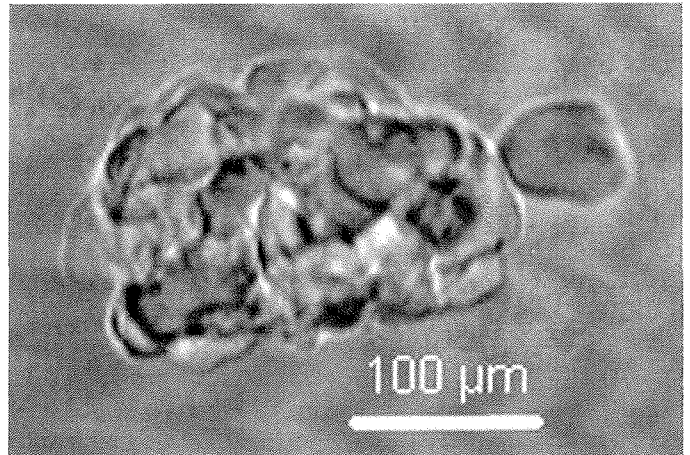


Fig. 2: Clathrate with cracks and grooves (depth: 1271 m).

Abb. 2: Clathrat mit Rissen und Rillen (Tiefe: 1271 m).

4) Clathrates after segregation

On further ice deformation, the splinters segregate and form individual clathrates of significantly smaller size. As can be seen in Figure 4, these are still translucent, so they have not metamorphosed into transparent secondary clathrates.

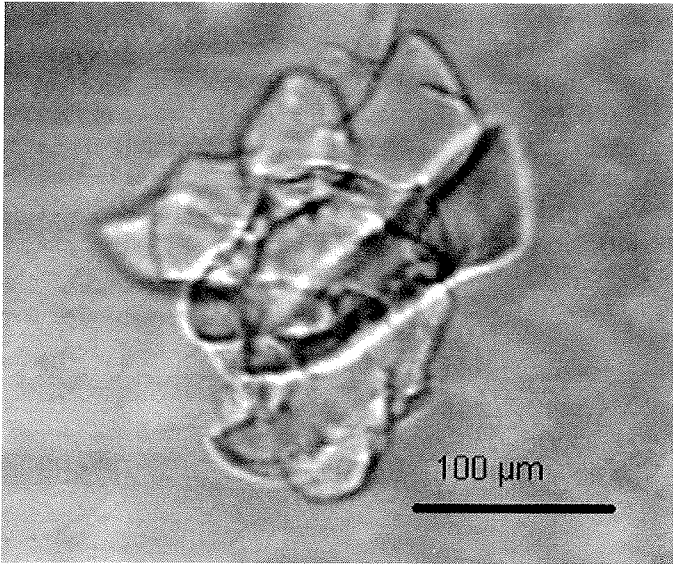


Fig. 3: Splintered clathrate (depth: 1271 m).

Abb. 3: Zersplittertes Clathrat (Tiefe: 1271 m).

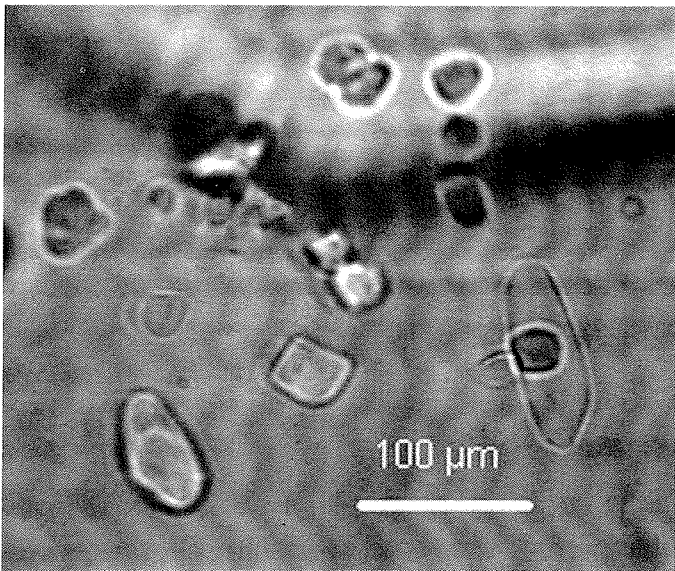


Fig. 4: Clathrate splinters have moved apart (depth 1352 m).

Abb. 4: Clathratsplitter, die sich voneinander entfernt haben (Tiefe: 1352 m).

SECONDARY CLATHRATES

Metamorphosis of clathrates

In Figure 5, a protrusion with straight edges evolves from the main body of a graupel-like primary clathrate. Presumably, a recrystallisation process takes place, involving decomposition of the primary clathrate cages, which leads to the transport of air molecules released from the primary part of the clathrate and cage reconstruction employing water molecules from the surrounding ice matrix. The next step of this process might be a

rod as shown in Figure 6 with a graupel-like central clathrate phase. It is noteworthy that this graupel-like phase is considerably smaller than the primary clathrates presented in Figures 1-3, with a diameter of ca. 50 µm.

The final stage of the metamorphosis might be a rod as presented in Figure 8. Due to ice deformation, a long, thin rod-like specimen presented here breaks up into smaller specimens, which eventually move apart and show up as individual small round or oval clathrates (Fig. 7).

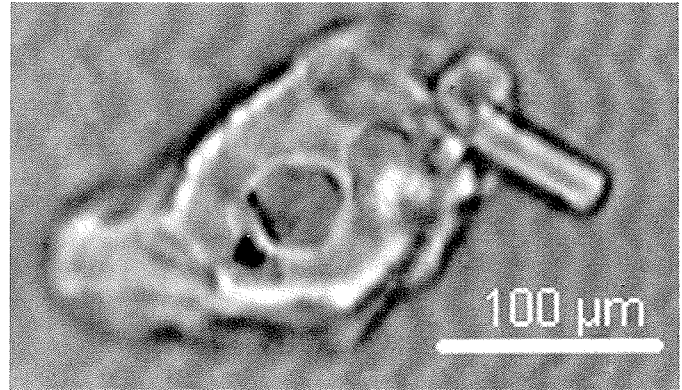


Fig. 5: Primary clathrate with a rod-like protrusion (depth: 1271 m).

Abb. 5: Primäres Clathrat mit einem stäbchenförmigen Auswuchs (Tiefe: 1271 m).

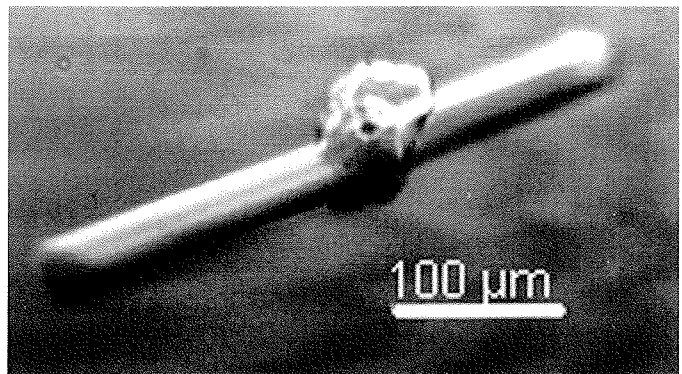


Fig. 6: Rod-like clathrate with a graupel-like centre (depth: 1378 m).

Abb. 6: Stäbchenförmiges Clathrat mit einem graupeligen Zentrum (Tiefe: 1378 m).

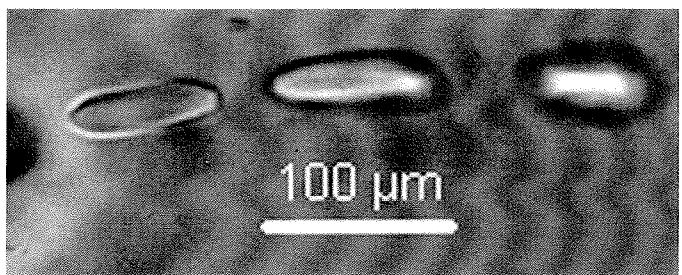


Fig. 7: Links after a rod-like clathrate has been cut into sub-units (depth: 1639 m).

Abb. 7: Untereinheiten eines ehemals stäbchenförmigen Clathrats (Tiefe: 1639 m).

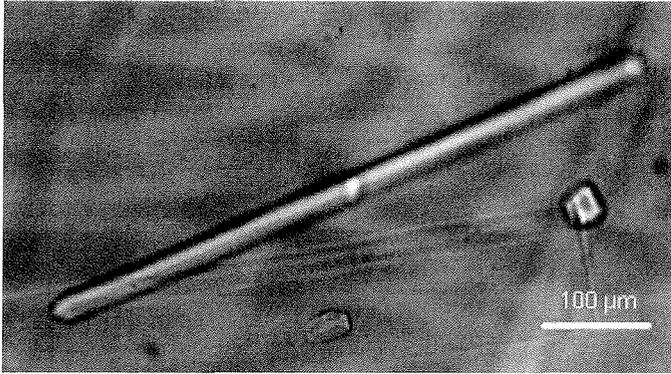


Fig. 8: Rod-like clathrate (completed transformation; depth: 1378 m).

Abb. 8: Stäbchenförmiges Clathrat (Umwandlung abgeschlossen; Tiefe: 1378 m).

1) Rod-like clathrates

The rod-like crystal in Figure 8 features a highlighted area in its centre, which supports the assumption of a metamorphosis process as described above. Its shape bears no resemblance to a primary clathrate or any air bubble encountered at the beginning of the transition zone. This is why a clathrate transformation is the only process accounting for the existence of this shape. In contrast to elongated spheroid (see below), rod-like clathrate have straight, parallel edges.

2) Faceted clathrates

Unlike primary clathrates with rough and curved surfaces, secondary clathrates often show clear and planar faces. These are considered to represent the faces of the cubic structure, or they are the result of the competitive energies of the different lattices of the cubic clathrate and the hexagonal ice matrix.

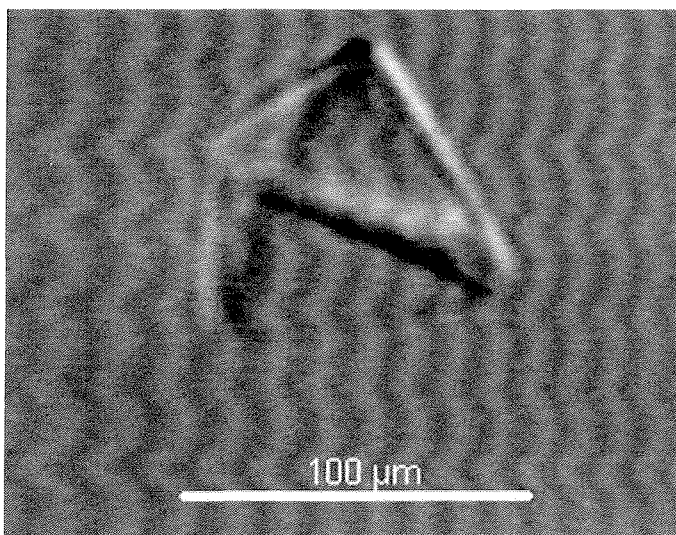


Fig. 9: Tetrahedral clathrate (depth: 1378 m).

Abb. 9: Tetraedrisches Clathrat (Tiefe: 1378 m).

a) Tetrahedral clathrates

A tetrahedron is a body composed of the four planes defined by $\{111\}$, and its -43 m equivalents of the cubic lattice of the clathrate ($\{-111\}$, $\{1-11\}$, and $\{11-1\}$). More often than a perfect tetrahedral shape as shown in Figure 9 we find specimens with capped apices, so that often we find triangular inclusions corresponding to the trigonal base of a tetrahedron. Bipyramidal specimens, most of which are capped, are also encountered.

b) Octahedral clathrates

Likewise, an octahedron consists of eight faces, which correspond to the $\{111\}$ planes in a cube and its crystallographic ($m-3m$) equivalents.

In this category, we also group clathrates that have the same hexagonal shape as platelet-like inclusions, also termed "inverse crystals" or "voids", which are optically distinguished from clathrates in that their edges do not brighten up in transmitted light in the microscope when slightly out of focus (Becke test; SHOJI & LANGWAY 1982), as can be seen in Figure 11. Considering that clathrates are reported to be harder than ice Ih (SALAMATIN et al. 1998), we assume that hexagonally shaped clathrates are thin cross sections of an octahedron rather than the result of the hexagonal ice matrix imposing its geometry on the clathrate inclusion.

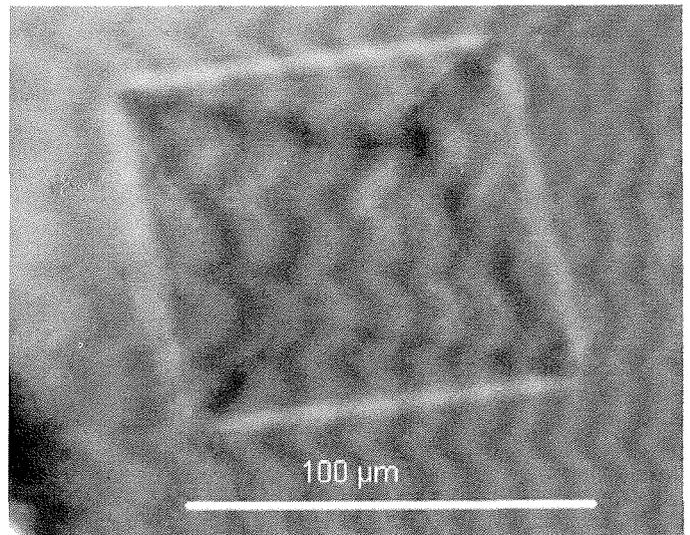


Fig. 10: Octahedral clathrate (depth: 1271 m).

Abb. 10: Oktaedrisches Clathrat (Tiefe: 1271 m).

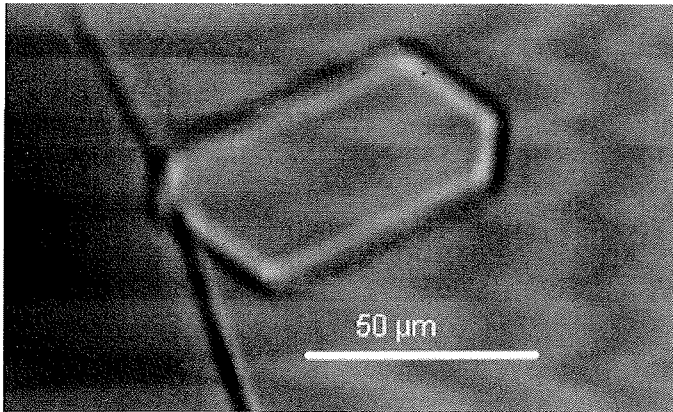


Fig. 11: Hexagonal clathrate (depth: 1271 m).

Abb. 11: Hexagonales Clathrat (Tiefe: 1271 m).

c) Poly-faceted clathrates

A relatively great proportion (about 5% on average) of clathrates at greater depth levels features planar faces with no regular geometry. They might be the result of a combination of different geometric patterns, such as tetrahedrons, octahedrons, hexagons, as the boundary surfaces are the result of hydrostatic forces and flow patterns of the ice matrix, so that crystals based on single geometric patterns are the exception rather than the rule.

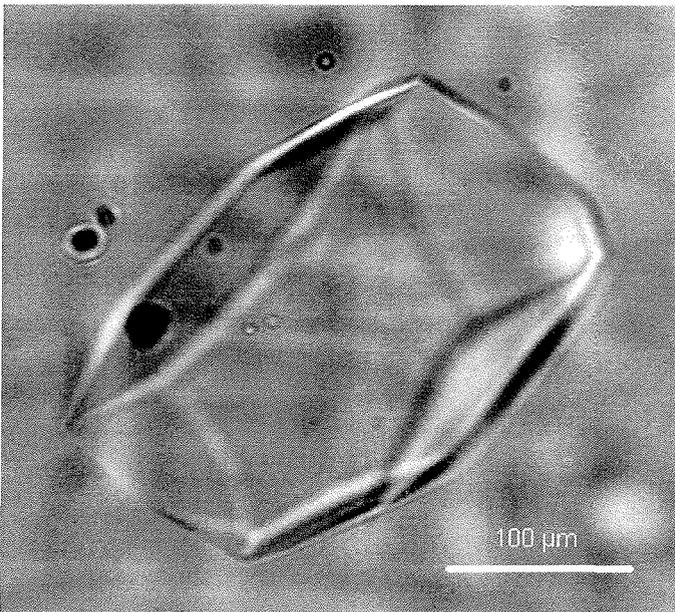


Fig. 12: Poly-faceted clathrate (depth: 1639 m).

Abb. 12: Polyfacettiertes Clathrat (Tiefe: 1639).

3) Spheroid clathrates

a) Spherical clathrates

The proportion of spherical secondary clathrates (Fig. 13) increases with depth. Although right below the transition zone the contribution of round clathrates to the total number is about 60 % already, its proportion rises to ca. 80 % at depths close to the bedrock. We assume that their shape is the result of competing forces of different lattice resulting in a minimised surface energy.

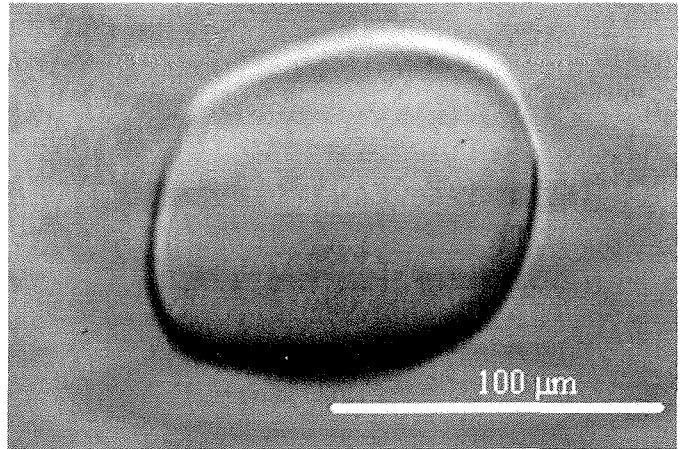


Fig. 13: Spherical clathrate (depth: 1639 m).

Abb. 13: Kugelförmiges Clathrat (Tiefe: 1639).

b) Ellipsoidal (elongated) clathrates

The distinction between spherical and ellipsoidal clathrates is somewhat arbitrary in that it is based on a definition of the ratio of the longest and the shortest dimension measured in the microscopic image of the clathrate. For a statistical representation of the number, size, and shape distribution of clathrates in the GRIP ice core (PAUER et al. 1999), we defined spheroid clathrates with a ratio (longest/shortest dimension) of greater than two belonging to the category 'elongated', as exemplified in Figure 14, those with a smaller ratio to the "spherical" type. In this statistical study we showed that the proportion of spherical clathrates increases on the way down at the expense of elongated clathrates, which means that clathrates get rounder the deeper they get.

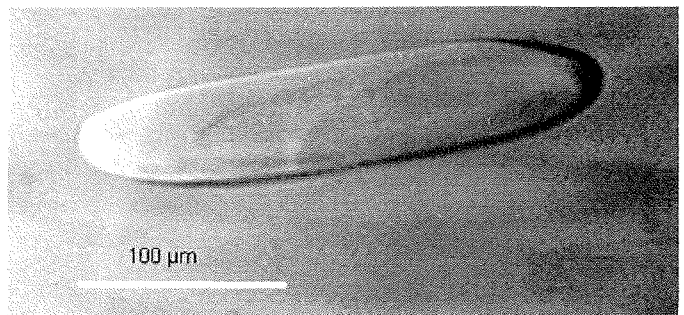


Fig. 14: Ellipsoidal clathrate (depth: 1309 m).

Abb. 14: Ellipsoidisches Clathrate (Tiefe: 1309 m).

MIXED TYPES AS RESULTS OF DIFFERENT CATEGORIES

In many cases, an individual clathrate specimen is the result of different processes. If, for instance, segregation and metamorphosis take place simultaneously, or if a clathrate is in the middle of a transformation process, the resulting crystal will not fit into the categories described above. This is why we consider it desirable to have a distinct category for miscellaneous clathrates. As these are combinations of several of the above, a further distinction would be tedious, and for statistical purposes, it would suffice to count them as "miscellaneous". From our collection of clathrate images, we present a few examples of the multitude of conceivable transition states and combination of features.

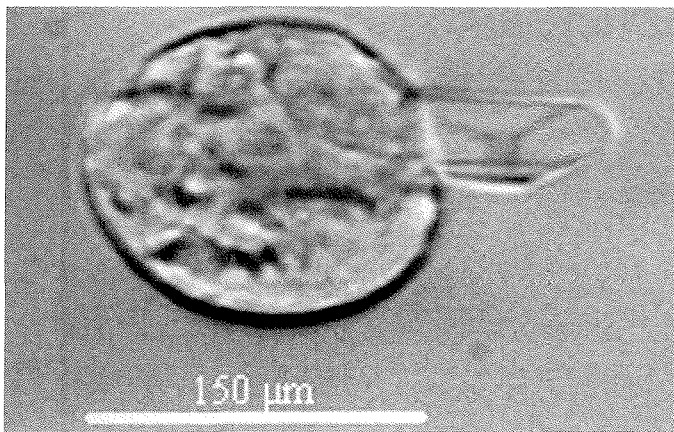


Fig. 15: Graupel-like clathrate with a nucleus of a rod (beginning of metamorphosis, depth: 1378 m).

Abb. 15: Graupeliges Clathrat mit einem stäbchenförmigen Keim (Beginn der Metamorphose; 1378 m).

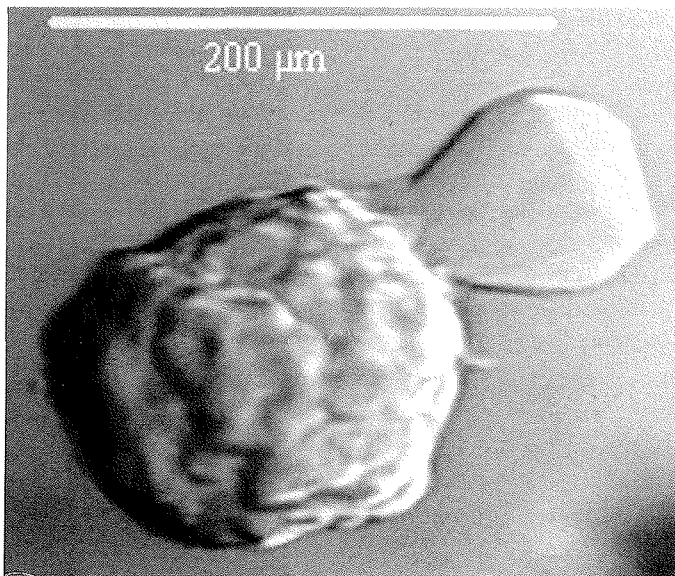


Fig. 16: Graupel-like clathrate metamorphosing into a poly-faceted clathrate (depth: 1378 m).

Abb. 16: Graupeliges Clathrat, das sich in ein polyfacettiertes umwandelt (Tiefe: 1378 m).

Figures 15 and 16 show a graupel-like, round clathrate with a

protrusion forming a rod-like specimen and a graupel-like clathrate metamorphosing into a poly-faceted clathrate, respectively. Both clathrates are comparable to that presented in Figure 5 and are examples of two-phase combinations in a transition state from primary to secondary clathrate.

A long unit divided into three poly-faceted sub-units (Fig. 17) is considered the result of a recrystallising rod-like clathrate which has split into three links.

A conglomeration of different clathrates in Figure 18, all showing curves and faces, might be the result of segregation after metamorphosis (cf. Fig. 17), with partly rounded edges.

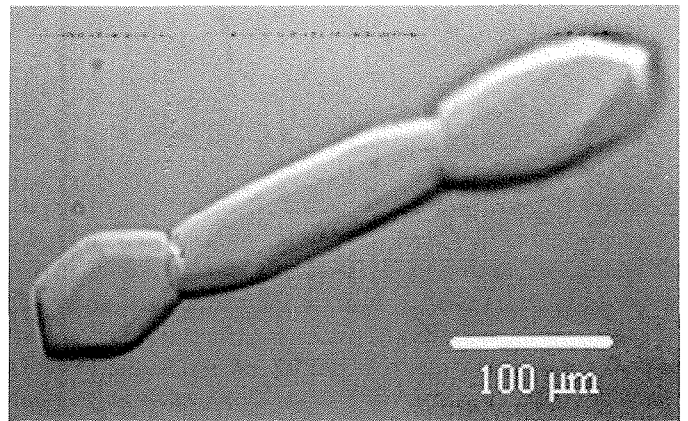


Fig. 17: Long poly-faceted clathrate dividing into links (depth: 1378 m).

Abb. 17: Langes polyfacettiertes Clathrat, das sich in Untereinheiten aufteilt (Tiefe: 1378 m).

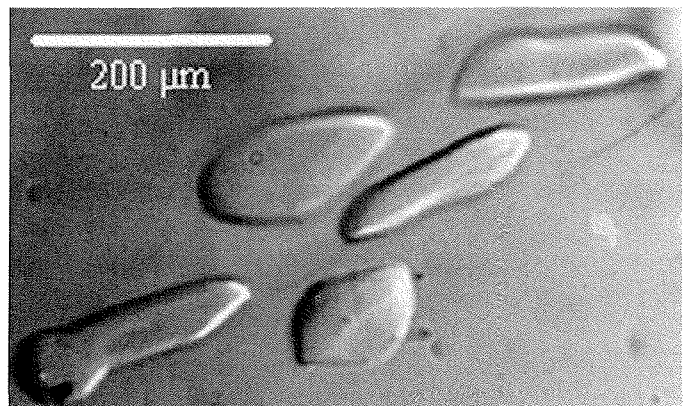


Fig. 18: Conglomeration of transparent clathrates, partly faceted (depth: 1513 m).

Abb. 18: Konglomerat von transparenten, teilweise facettierten Clathraten (Tiefe: 1513 m).

A primary clathrate with faces and protrusions, not encountered frequently, can be seen in Fig. 19. As transparent crystals, straight edges, and plane faces are the features of secondary clathrates, it is doubtful that this specimen actually has an octahedral body, as might be suggested in the picture. Again, the protrusions are considered the result of a recrystallisation process (metamorphosis) as can be seen by their greater level of transparency.

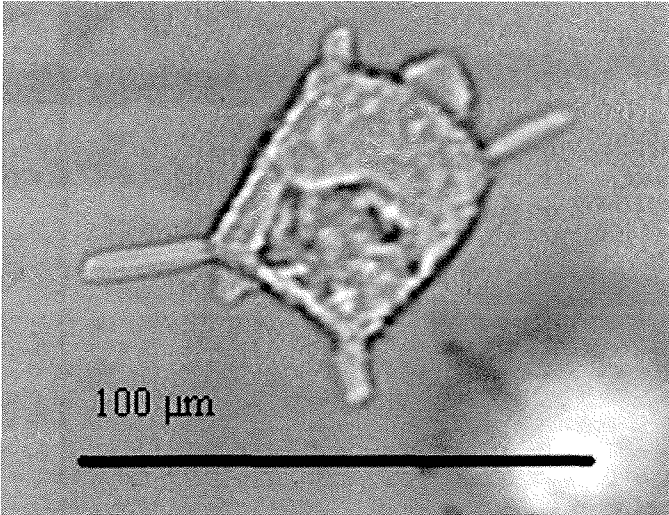


Fig. 19: Graupel-like clathrate with several protrusions (depth: 1331 m).

Abb. 19: Graupelförmiges Clathrat mit diversen Auswüchsen (Tiefe: 1331 m).

Rod-like clathrates featuring a round tip might be the result of a metamorphosis of the remaining fraction of a clathrate after a great proportion has grown into a rod. Unlike the situation in Figures 15 and 16, the round tip shows facets and straight edges, thus suggesting the secondary nature of this part of the clathrate.

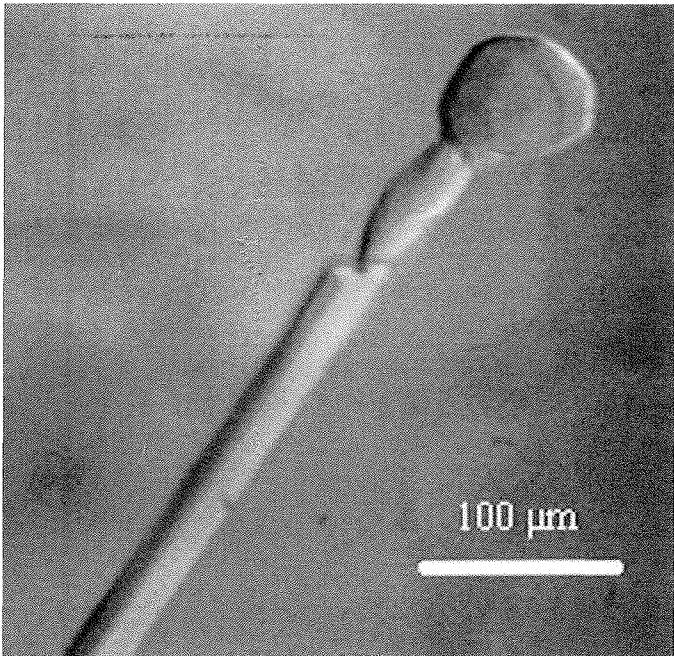


Fig. 20: Rod-like clathrate ending in a poly-faceted ball-like tip (depth: 1513 m).

Abb. 20: Stäbchenförmiges Clathrat, das in einer kugelförmigen Spitze endet (Tiefe: 1513 m).

A faceted clathrate with a rounded edge can be seen in Figure 21. It is not clear why one side of the clathrate features facets and sharp edges, whereas the other is rounded off.

To account for the diversity of shapes and different transition states we have classified these as miscellaneous, or mixed, clathrates.

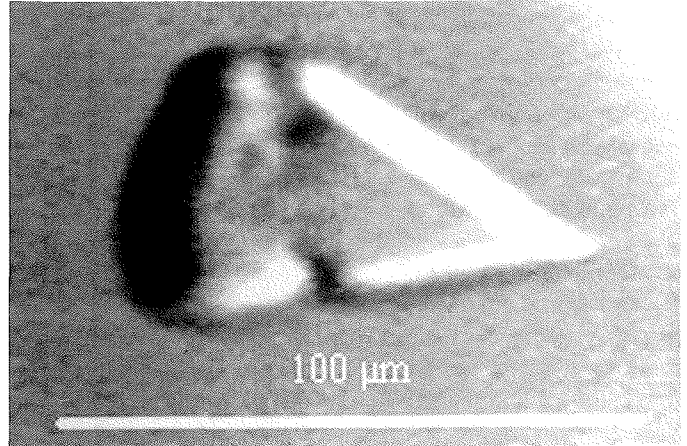


Fig. 21: Wedge-shaped clathrate with faceted edges (depth: 1639 m).

Abb. 21: Keilförmiges Clathrat mit facettierten Kanten (Tiefe: 1639 m).

CONCLUSION

We have classified natural air clathrates in polar ice sheets into subcategories that are meant to simplify and standardise the cri-

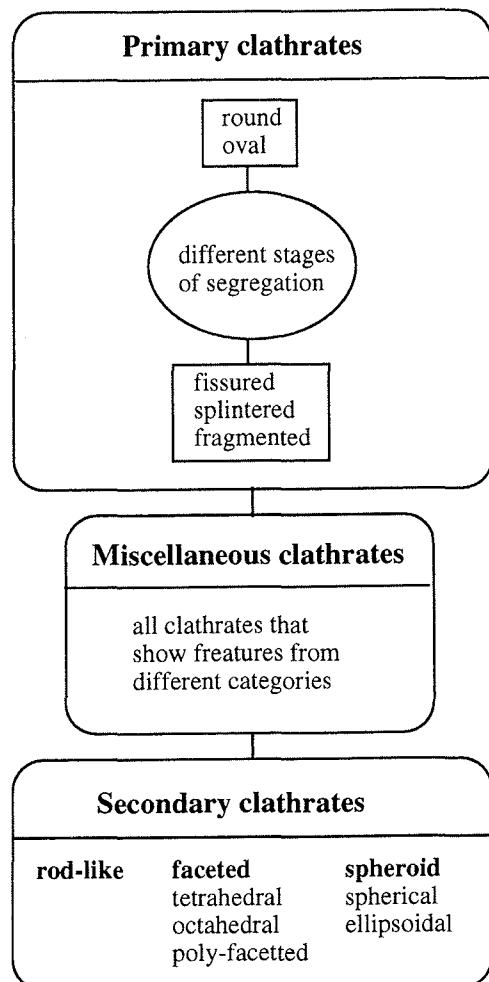


Fig. 22: Natural air clathrate classification scheme.

Abb. 22: Klassifizierungs-Schema für natürliche Luft-Clathrate

teria for a general classification of clathrate morphology. Yet because of the overlap of different dimensions of classification (stage of formation vs. morphological aspects) it is sometimes difficult to assign a given clathrate specimen to one of the above categories. For statistical purposes, however, this would not be significant, and, with respect to the processes involving clathrates and air distribution in polar ice sheets, a distinction between basic categories, such as "primary" and "secondary" clathrates, and, in order to document the influence of ice sheet dynamics on clathrate morphology, between subcategories, such as rod-like, poly-faceted, and spheroid, helps establish a framework for the interpretation of clathrate transformation stages. The classification scheme is summarized in the diagram of Figure 22.

ACKNOWLEDGEMENTS

This work is a contribution to the North Greenland Ice core Project (NGRIP). This paper is contribution No. 1731 of the Alfred-Wegener-Institute, Bremerhaven, Germany.

References

- Hondoh, T. (1996): Clathrate hydrates in polar ice sheets.- Proc. Second International Conference on Natural Gas Hydrates, 2-6 June 1996, Toulouse, ENSIGC-INPT, 131-138.
- Kipfstuhl, S., Pauer, F., Kuhs, W.F. & Shoji, H. (submitted): Air bubbles and clathrates in the transition zone of the NGRIP deep ice core.- Geoph. Res. Lett.
- Kuhs, W.F., Techmer, K., Klapproth, A., Gotthard, F. & Heinrichs, T. (in press): First observation of mesoporous gas hydrates.- Geoph. Res. Lett.
- Miller, S.L. (1969): Clathrate hydrates of air in Antarctic ice.- Science 165: 489-490.
- Narita, H., Azuma, N., Hondoh, T., Fuji, M., Kawaguchi, M., Mae, S., Shoji, H., Kameda, T. & Watanabe O. (1999): Characteristics of air bubbles and hydrates in the Dome Fuji ice core, Antarctica.- Ann. Glaciol. 29: 207-210.
- Pauer, F., Kipfstuhl, J., Kuhs, W.F. & Shoji, H. (1999): Air clathrate crystals from the GRIP deep ice core, Greenland: a number-, size and shape-distribution study.- J. Glaciol. 45 (149): 22-30.
- Salamatin, A.N., Hondoh, T., Uchida, T. & Lipenkov, V.Ya. (1998): Post-nucleation conversion of an air bubble to clathrate hydrate crystal in ice.- J. Cryst. Growth 193: 197-218.
- Shoji, H. & Langway Jr., C.C. (1982): Air hydrate inclusions in fresh ice core.- Nature 298: 548-550.
- Stackelberg, M. von & Müller, H.R. (1954): Feste Gashydrate II.- Z. Elektrochem. 58: 25-39.
- Uchida, T., Hondoh, T., Mae, S., Lipenkov, V.Ya. & Duval, P. (1994): Air-hydrate crystals in deep ice-core sample from Vostok Station, Antarctica.- J. Glaciol. 40 (134): 79-86.